Frequency-domain Bernstein-Bézier finite element solver for modelling short waves Part I - Application to elastic wave simulations

N. Benatia[1], A. El Kacimi[1], O. Laghrouche[2], M. El Alaoui Talibi[3], J. Trevelyan[4]

[1]Cadi Ayyad University, [2]Heriot-Watt University, [3]Mohammed VI Polytechnic, [4]Durham University

Outline

Motivation

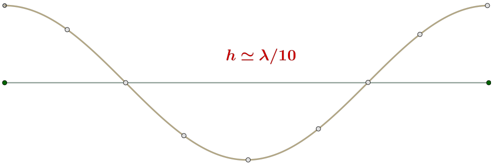

When solving short wave problems stated in unbounded domains by FEM, the main challenges are:

- The pollution error: the relative *hp*-FE error for Helmholtz problems in the H^1-seminorm, on a uniform hp-mesh, is bounded by

$$\frac{|u-u_h|_1}{|u|_1} \leq C_1 \left(\frac{kh}{2p}\right)^p + C_2 k \left(\frac{kh}{2p}\right)^{2p}$$

- The truncation of the infinite domain
- The accurate representation of curved geometries

Time-harmonic elastic wave equation

We consider an isotropic linear homogeneous elastic medium into a domain $\Omega \subset \mathbb{R}^2$ and $\Gamma = \partial\Omega$ denoting the boundary of Ω;

Time-harmonic elastic wave problem consists of finding a function $\boldsymbol{u} : \Omega \to \mathbb{C} \times \mathbb{C}$ satisfying

$$\begin{cases} -\rho\omega^2 \boldsymbol{u} - \boldsymbol{\nabla} \cdot \boldsymbol{\sigma}(\boldsymbol{u}) = 0 \quad \text{in} \quad \Omega, \\ \boldsymbol{\sigma}(\boldsymbol{u})\boldsymbol{n} = \mathrm{i}\left[\dfrac{E(1-\nu)}{(1+\nu)(1-2\nu)} k_P (\boldsymbol{u}\cdot\boldsymbol{n})\boldsymbol{n} + \dfrac{E}{2(1+\nu)} k_S (\boldsymbol{u}\cdot\boldsymbol{t})\boldsymbol{t}\right] + \boldsymbol{g} \quad \text{on} \quad \Gamma. \end{cases}$$

where

- $\rho > 0$ is the (constant) material density and ω is the circular frequency
- ν and E are the Poisson's ratio and Young's modulus, respectively (also constant)
- $\boldsymbol{g}$ is a source term, with $\boldsymbol{n}$ and $\boldsymbol{t}$ denoting the outward unit normal and tangent vectors to Γ
- k_P and k_S are the compressional (P) and shear (S) wave numbers, given by

$$k_P = \omega\sqrt{\frac{\rho(1+\nu)(1-2\nu)}{E(1-\nu)}} \quad \text{and} \quad k_S = \omega\sqrt{\frac{2\rho(1+\nu)}{E}}$$

Hooke's law:

$$\boldsymbol{\sigma}(\boldsymbol{u}) = \frac{E\nu}{(1+\nu)(1-2\nu)}\left(\boldsymbol{\nabla}\cdot\boldsymbol{u}\right)\boldsymbol{I} + \frac{E}{2(1+\nu)}\left(\boldsymbol{\nabla}\boldsymbol{u} + \boldsymbol{\nabla}\boldsymbol{u}^\top\right)$$

Variational formulation

To derive a variational formulation for the time harmonic elastic problem, the following usual Sobolev space $\boldsymbol{V} = H^1(\Omega) \times H^1(\Omega)$ is introduced.
Let us multiply by the complex conjugate of a test function $\boldsymbol{v} \in \boldsymbol{V}$, integrating by parts over Ω , and using the well known identity

$$\boldsymbol{\sigma}(\boldsymbol{u}) \cdot \boldsymbol{\nabla}\bar{\boldsymbol{v}} = \frac{E\nu}{(1+\nu)(1-2\nu)}(\boldsymbol{\nabla}\cdot\boldsymbol{u})(\boldsymbol{\nabla}\cdot\bar{\boldsymbol{v}}) + \frac{E}{(1+\nu)}\boldsymbol{\nabla}\boldsymbol{u}\cdot\boldsymbol{\nabla}\bar{\boldsymbol{v}} - \frac{E}{2(1+\nu)}(\boldsymbol{\nabla}\times\boldsymbol{u})(\boldsymbol{\nabla}\times\bar{\boldsymbol{v}}),$$

and taking into account the b.c., yields the following weak form:

$$\begin{cases} \text{Find } \boldsymbol{u} \text{ in } \boldsymbol{V} \text{ such that} \\ -\omega^2\rho \displaystyle\int_\Omega \boldsymbol{u}\cdot\bar{\boldsymbol{v}}\, d\Omega + \frac{E\nu}{(1+\nu)(1-2\nu)}\int_\Omega (\boldsymbol{\nabla}\cdot\boldsymbol{u})(\boldsymbol{\nabla}\cdot\bar{\boldsymbol{v}})\, d\Omega \\ +\displaystyle\frac{E}{(1+\nu)}\int_\Omega \boldsymbol{\nabla}\boldsymbol{u}\cdot\boldsymbol{\nabla}\bar{\boldsymbol{v}}\, d\Omega - \frac{E}{2(1+\nu)}\int_\Omega (\boldsymbol{\nabla}\times\boldsymbol{u})(\boldsymbol{\nabla}\times\bar{\boldsymbol{v}})\, d\Omega \\ -\mathrm{i}\displaystyle\int_\Gamma \left[\frac{E(1-\nu)}{(1+\nu)(1-2\nu)}k_P(\boldsymbol{u}\cdot\boldsymbol{n})(\bar{\boldsymbol{v}}\cdot\boldsymbol{n}) + \frac{E}{2(1+\nu)}k_S(u\cdot\boldsymbol{t})(\bar{\boldsymbol{v}}\cdot\boldsymbol{t})\right] d\Gamma = \int_\Gamma \boldsymbol{g}\cdot\bar{\boldsymbol{v}}\, d\Gamma, \\ \text{for all } \boldsymbol{v} \text{ in } \boldsymbol{V}. \end{cases}$$

Existence and uniqueness :

Gårding's inequality $\longrightarrow$ Fredholm's alternative $+$ continuation arguments

Reference triangle $\hat{T}$

Barycentric coordinates and the linear blending map of Gordon & Hall

Let $\hat{T}$ the reference element defined by,

$$\hat{T} := \{\xi = (\xi_1, \xi_2) \in \mathbb{R}^2 : \quad 0 \leq \xi_1 \leq 1, \quad 0 \leq \xi_2 \leq 1 - \xi_1\}.$$

The barycentric coordinates relative to the reference element:

$$\lambda_1(\xi_1, \xi_2) = \xi_1, \quad \lambda_2(\xi_1, \xi_2) = \xi_2, \quad \lambda_3(\xi_1, \xi_2) = 1 - \xi_1 - \xi_2.$$

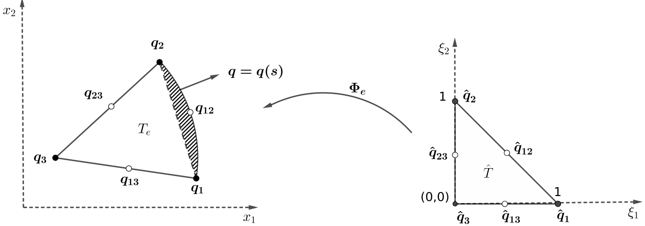

Let consider the case of a triangular element with only one curved edge and assume it is edge $e_1 = (\boldsymbol{q}_1\ \boldsymbol{q}_2)$, given by its parametric form $\boldsymbol{q} = \boldsymbol{q}(s)$, where $0 \leq s \leq 1$, $\boldsymbol{q}(0) = \boldsymbol{q}_1$ and $\boldsymbol{q}(1) = \boldsymbol{q}_2$. A map denoted Φ_e and defined from $\hat{T}$ to T_e can be written as

$$\Phi_e(\boldsymbol{\xi}) = \lambda_1(\boldsymbol{\xi})\boldsymbol{q}_1 + \lambda_2(\boldsymbol{\xi})\boldsymbol{q}_2 + \lambda_3(\boldsymbol{\xi})\boldsymbol{q}_3 + \frac{\lambda_1(\boldsymbol{\xi})\lambda_2(\boldsymbol{\xi})}{\xi_2(1-\xi_2)}\left[\boldsymbol{q}(\xi_2) - ((1-\xi_2)\boldsymbol{q}_1 + \xi_2\boldsymbol{q}_2)\right].$$

Bernstein polynomial basis on reference triangle $\hat{T}$

- Vertex based shape functions

$$\phi_1^v(\boldsymbol{\xi}) = \lambda_1^{p^{v_1}}(\boldsymbol{\xi}), \quad \phi_2^v(\boldsymbol{\xi}) = \lambda_2^{p^{v_2}}(\boldsymbol{\xi}), \quad \phi_3^v(\boldsymbol{\xi}) = \lambda_3^{p^{v_3}}(\boldsymbol{\xi});$$

- Edge based shape functions

$$\phi_k^{e_1}(\boldsymbol{\xi}) = \binom{p^{e_1}}{k} \lambda_1^{p^{e_1}-k}(\boldsymbol{\xi})\lambda_2^k(\boldsymbol{\xi}), \quad 1 \leqslant k \leqslant p^{e_1} - 1;$$

$$\phi_k^{e_2}(\boldsymbol{\xi}) = \binom{p^{e_2}}{k} \lambda_2^{p^{e_2}-k}(\boldsymbol{\xi})\lambda_3^k(\boldsymbol{\xi}), \quad 1 \leqslant k \leqslant p^{e_2} - 1;$$

$$\phi_k^{e_3}(\boldsymbol{\xi}) = \binom{p^{e_3}}{k} \lambda_3^{p^{e_3}-k}(\boldsymbol{\xi})\lambda_1^k(\boldsymbol{\xi}), \quad 1 \leqslant k \leqslant p^{e_3} - 1;$$

- Bubble based shape functions

$$\phi_{ij}^b(\boldsymbol{\xi}) = \binom{p^b}{i+j}\binom{i+j}{i} \lambda_1^i(\boldsymbol{\xi})\lambda_2^j(\boldsymbol{\xi})\lambda_3^{p^b-i-j}(\boldsymbol{\xi}), \quad 1 \leqslant i+j \leqslant p^b - 1;$$

$$\binom{m}{k} := \frac{m!}{k!(m-k)!}.$$

Approximation by BBFEM

The approximated Bernstein-Bézier FE solution of the displacement field, denoted by $\boldsymbol{u}_h$, can be written element-wise in the form

$$\boldsymbol{u}_h(\boldsymbol{x}) = \sum_{i=1}^{3} \phi_i^v(\boldsymbol{\xi})\boldsymbol{u}_i^v + \sum_{k=1}^{3}\sum_{i=1}^{p-1} \phi_i^{e_k}(\boldsymbol{\xi})\boldsymbol{u}_i^{e_k} + \sum_{1\leqslant i+j\leqslant p-1} \phi_{ij}^b(\boldsymbol{\xi})\boldsymbol{u}_{ij}^b$$

where $\boldsymbol{u}_i^v, \boldsymbol{u}_i^{e_k}, \boldsymbol{u}_{ij}^b \in \mathbb{C}^2$ are the unknown column vectors.

- Bernstein polynomials form a partition of unity $(p^v = p^e = p^b = p)$
- Analytical rules apply in the case of constant coefficients and affine elements

Bernstein polynomial basis on reference triangle $\hat{T}$

The key technique to obtain a good performance from BBFEM is the use of static condensation:

- Remove interior modes from the resulting discrete algebraic system during the assembling process;
- Recover interior modes by solving small linear algebraic systems at an elemental level;

For a polynomial order $p \geq 3$, the number of DoF per element is given by

$$n^e_{dof} = 6 + 6(p-1) + (p-1)(p-2)$$

Static condensation (Shur complement) is performed at the elemental level;
b = boundary modes, i = interior modes

$$\left(\begin{array}{c|c} \boldsymbol{A}^e_{b,b} & \boldsymbol{A}^e_{b,i} \\ \hline \boldsymbol{A}^e_{i,b} & \boldsymbol{A}^e_{i,i} \end{array}\right) \left(\begin{array}{c} \boldsymbol{U}^e_b \\ \hline \boldsymbol{U}^e_i \end{array}\right) = \left(\begin{array}{c} \boldsymbol{F}^e_b \\ \hline \boldsymbol{F}^e_i \end{array}\right) \Longrightarrow \begin{cases} \hat{\boldsymbol{A}}^e_b \boldsymbol{U}^e_b = \hat{\boldsymbol{F}}^e_b \\ \boldsymbol{U}^e_i = [\boldsymbol{A}^e_{i,i}]^{-1}(\boldsymbol{F}^e_i - \boldsymbol{A}^e_{i,b}\boldsymbol{U}^e_b) \\ \hat{\boldsymbol{A}}^e_b = \boldsymbol{A}^e_{b,b} - \boldsymbol{A}^e_{b,i}[\boldsymbol{A}^e_{i,i}]^{-1}\boldsymbol{A}^e_{i,b} \\ \hat{\boldsymbol{F}}^e_b = \boldsymbol{F}^e_b - \boldsymbol{A}^e_{b,i}[\boldsymbol{A}^e_{i,i}]^{-1}\boldsymbol{F}^e_i \end{cases}$$

$$\boldsymbol{A}^e_{i,i} \in \mathbb{C}^N \times \mathbb{C}^N, \ \ N = (p-1)(p-2)$$

Measures of performance

- The accuracy of BBFEM is assessed by the following L^2 error

$$\varepsilon_2 = \frac{\|\boldsymbol{u}_h - \boldsymbol{u}\|_{L^2(\Omega)}}{\|\boldsymbol{u}\|_{L^2(\Omega)}} \times 100\%.$$

- The wave resolution is measured by the parameter

$$\tau_S = \lambda_S \sqrt{\frac{n_{\text{dof}}}{|\Omega|}},$$

giving the numbers of DoF per λ_S. Here $|\Omega|$ is the surface area of Ω.

- The condition number is evaluated using the metric

$$\kappa = \frac{||\, |A|\, |A^{-1}|\, |\hat{x}| \; + \; |A^{-1}|\, |b|\, ||_\infty}{||\hat{x}||_\infty}.$$

Shear wave scattering

Description of the Benchmark

The first benchmark problem deals with the elastic wave scattering problem, in which an incident shear plane wave

$$\mathbf{u}^{\text{in}} = -ik_{\text{S}} \exp\left(ik_{\text{S}}x\right) \mathbf{e}_y$$

travelling from the left to the right along the horizontal direction and impinging on a circular rigid body of radius a.

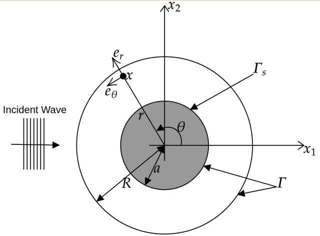

The analytical solution : (given in the polar coordinate system $(\boldsymbol{e}_r, \boldsymbol{e}_t)$)

$$\begin{aligned} u_r &= \sum_{\nu=0}^{\infty} \left(\varepsilon_\nu \mathrm{i}^\nu k_P \mathrm{J}'_\nu(k_P r) + k_P A_\nu \mathrm{H}'_\nu(k_P r) + \nu B_\nu \frac{\mathrm{H}_\nu(k_P r)}{r} \right) \cos(\nu\theta) \\ u_t &= \sum_{\nu=0}^{\infty} - \left(\varepsilon_\nu \mathrm{i}^\nu \nu \frac{\mathrm{J}_\nu(k_P r)}{r} + \nu A_\nu \frac{\mathrm{H}_\nu(k_P r)}{r} + B_\nu k_S \mathrm{H}'_\nu(k_S r) \right) \sin(\nu\theta), \end{aligned}$$

where

- J_ν and J'_ν are, respectively, the Bessel function of the first kind and order ν, and its first derivative.
- H_ν and H'_ν are, respectively, the Hankel function of the first kind and order ν, and its first derivative.
- The sequence $\{\varepsilon_\nu\}$ is defined by $\varepsilon_0 = 1$, and $\varepsilon_\nu = 2$ for all $\nu \geq 1$.
- The constants A_ν, B_ν are chosen such that $\boldsymbol{u} = 0$ on Γ_s.

Shear wave scattering

Contour plot

In this benchmark problem, for numerical experiments, the parameter a is taken equal to 1, and the elastic properties of the medium are taken to be those of Aluminum: $E = 69 \times 10^9 \mathrm{N/m}^2$, $\nu = 0.32$ and $\rho = 2700 \mathrm{kg/m}^3$, which corresponds to the shear waves speed $c_S = 3111.29 \mathrm{m/s}$.

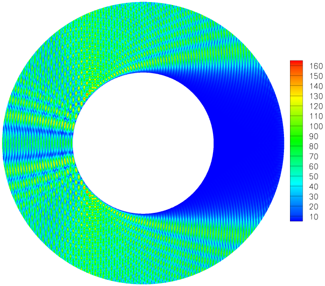

Figure: Contour plot of $|\mathrm{Re}(\boldsymbol{u}_h)|$ at $f = 4.0 \times 10^4 \mathrm{Hz}$.

Shear wave scattering

h-convergence analysis

To investigate the *h*-convergence analysis of BBFEM, a sequence of five gradually refined mesh grids are considered, with typical examples shown below.

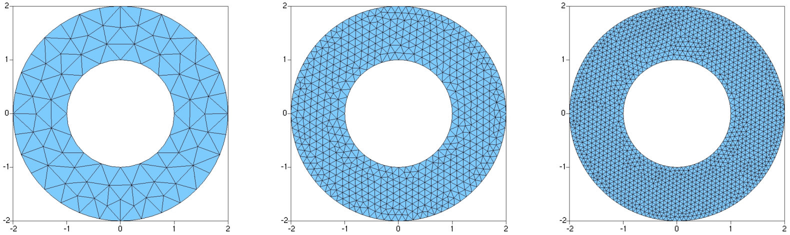

Figure: Examples of unstructured mesh grids used in the wave scattering problem; from left to right: M_1 $(h = 0.54a)$, M_3 $(h = 0.20a)$ and M_5 $(h = 0.13a)$.

Shear wave scattering

Error analysis: *h*-refinement

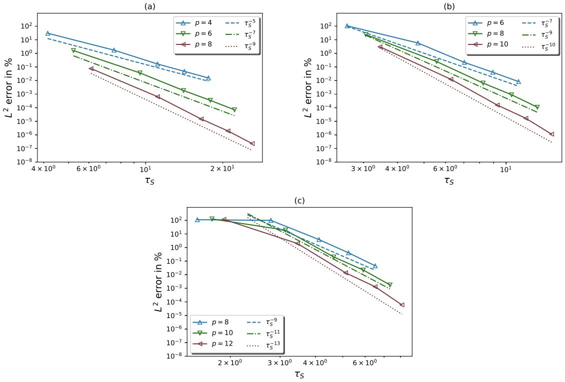

Figure: L^2 error versus τ_S (S wave stress); *h*-refinement for different values of the polynomial order p: (a) $f = 10,000$ Hz, (a) $f = 20,000$ Hz and (c) $f = 40,000$ Hz.

This method enables the recovery of an asymptotically algebraic decay of the L^2 error which scales as ${\tau_S}^{-p-1}$.

Shear wave scattering

Error analysis: *p*-refinement

All the numerical experiments are performed on mesh grid with $h = 0.20a$, with the frequencies 10,000Hz, 20,000Hz and 40,000Hz.

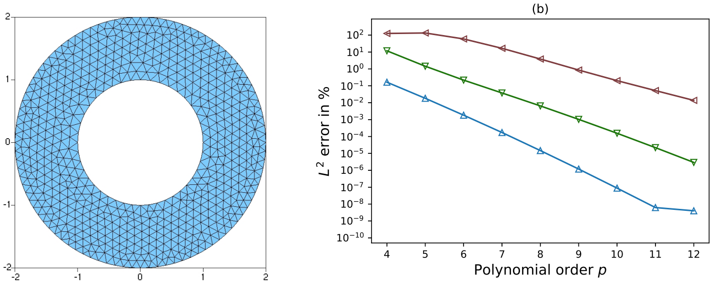

Figure: L^2 error versus the polynomial order for different frequencies; *p*-refinement with M_3 ($h = 0.20a$).

As expected, and since these benchmark tests make use of smooth analytical solutions, an exponential convergence is achieved.

Elastic transmission problem

Description of the Benchmark / p-adaptivity

Transmission of elastic plane waves through an inhomogeneous elastic cylinder with radius $r = a$, embedded in an infinite homogeneous elastic medium.

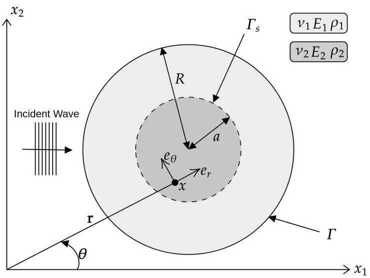

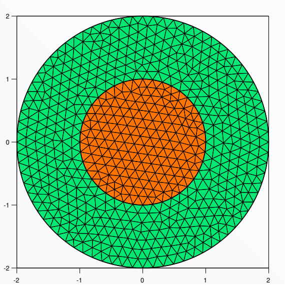

Use a p-adaptive analysis in which

$$\frac{k_S^{(1)} h_1}{p_1} \simeq \gamma \frac{k_S^{(2)} h_2}{p_2}, \quad \text{with} \quad \gamma = \frac{1}{2}\left(1 + \frac{k_S^{(2)}}{k_S^{(1)}}\right)$$

Elastic transmission problem

Description of the Benchmark

The analytical solution in this case is given in the polar coordinate system by

$$\begin{cases} \mathbf{u}_1 = \mathbf{u}_{1r}\mathbf{e}_r + u_{1\theta}\mathbf{e}_\theta \\ \mathbf{u}_2 = \mathbf{u}_{2r}\mathbf{e}_r + \mathbf{u}_{2\theta}\mathbf{e}_\theta \end{cases}$$

where

$$\mathbf{u}_{1r} = \sum_{m=0}^{+\infty} \left(-m\varepsilon_m i^m \frac{J_m(k_S^{(1)} r)}{r} + A_m k_P^{(1)} \dot{H}_m^{(1)}(k_P^{(1)} r) - mB_m \frac{H_m^{(1)}(k_S^{(1)} r)}{r} \right) \sin(m\theta)$$

$$\mathbf{u}_{1\theta} = \sum_{m=0}^{+\infty} \left(-\varepsilon_m i^m k_S^{(1)} J_m'(k_S^{(1)} r) + mA_m \frac{H_m^{(1)}(k_P^{(1)} r)}{r} - B_m k_S^{(1)} \dot{H}_m^{(1)}(k_S^{(1)} r) \right) \cos(m\theta)$$

$$\mathbf{u}_{2r} = \sum_{m=0}^{+\infty} \left(C_m k_P^{(2)} J_m'(k_P^{(2)} r) - mD_m \frac{J_m(k_S^{(2)} r)}{r} \right) \sin(m\theta)$$

$$\mathbf{u}_{2\theta} = \sum_{m=0}^{+\infty} \left(mC_m \frac{J_m(k_P^{(2)} r)}{r} - D_m k_S^{(2)} J_m'(k_S^{(2)} r) \right) \cos(m\theta)$$

where $k_{\mathrm{P}}^{(1)}$ and $k_{\mathrm{S}}^{(1)}$ are the compressional and shear wave numbers, respectively, in the medium. $k_{\mathrm{P}}^{(2)}$ and $k_{\mathrm{S}}^{(2)}$ are the compressional and shear wave numbers, respectively, in the cylinder.

Elastic transmission problem

p-adaptive analysis

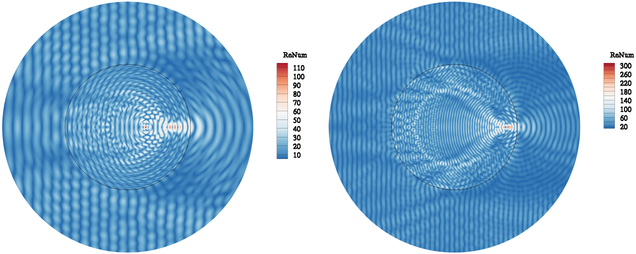

Figure: Contour plots of $|\mathrm{Re}(\boldsymbol{u}_h)|$ at $f = 4.0 \times 10^4$ Hz; elastic waves transmission; $\tau_S = 6.10$ and $k_S^{(2)}/k_S^{(1)} = 2$: (left) P incident wave, (right) S incident wave.

Elastic transmission problem

p-adaptive analysis

	Uniform p-refinement					Non uniform p-refinement				
f	p	n_{dof}	nnz	$\varepsilon_2[\%]$	κ_A	(p_1, p_2)	n_{dof}	nnz	$\varepsilon_2[\%]$	κ_A
10 kHz	4	12,206	262,589	5.75	0.99e+4	(3,4)	9,702	180,369	6.47	0.95e+4
	6	19498	610779	3.07e-3	0.14e+5	(4,6)	14490	372723	1.19e-2	0.11e+5
	8	26,790	1,102,377	2.07e-5	0.25e+5	(5,8)	19,278	634,869	1.85e-4	0.18e+5
	10	34,082	1,737,383	1.32e-6	0.10e+6	(7,10)	26,570	1,123,283	1.05e-6	0.10e+6
	12	41,374	2,515,797	5.50e-6	0.10e+7	(8,12)	31,358	1,549,765	9.63e-8	0.10e+7
20 kHz	4	12,206	262,589	97.25	0.24e+4	(3,4)	9,702	180,369	97.28	0.20e+4
	6	19,498	610,779	0.75	0.25e+4	(4,6)	14,490	372723	0.75	0.25e+4
	8	26,790	1,102,377	1.07e-2	0.61e+4	(5,8)	19,278	634,869	1.07e-2	0.59e+4
	10	34,082	1,737,383	2.92e-4	0.57e+5	(7,10)	26,570	1,123,283	2.92e-4	0.57e+5
	12	41,374	2,515,797	6.38e-6	0.73e+6	(8,12)	31,358	1,549,765	6.30e-6	0.73e+6
40 kHz	8	26,790	1,102,377	72.77	0.55e+6	(5,8)	19,278	634,869	72.66	0.55e+6
	10	34,082	1,737,383	2.27	0.58e+6	(7,10)	26,570	1,123,283	2.27	0.58e+6
	12	41,374	2,515,797	5.51e-2	0.10e+8	(8,12)	31,358	1,549,765	5.51e-2	0.10e+8
	14	48,666	3,437,619	3.11e-3	0.19e+9	(9,14)	36,146	2,046,039	3.52e-3	0.19e+9

Table: S-wave scattering, $k_S^{(2)}/k_S^{(1)} = 4$.

Thank you!

Continued talk

Part II - Bernstein-Bézier *H(curl)*–conforming FEM efficient solver for time-harmonic electromagnetic wave problems in media with interfaces